Hazard and Impact Knowledge for Europe

Deliverable 3.5

Final case study report on seismicity and safety of subsurface injection, Rousse, France

Authors and affiliation:
Hideo Aochi [BRGM]

E-mail of lead author:
h.aochi@brgm.fr

Version: 2021.10.14

This report is part of a project that has received funding by the European Union's Horizon 2020 research and innovation programme under grant agreement number 731166. Scientific work is co-funded by the Geological Surveys and national funds allocated for science within the period 2018-2021.

Deliverable Data		
Deliverable number	D3.5	
Dissemination level	Public	
Deliverable name	Final case study report on seismicity and safety of subsurface injection, Rousse, France	
Work package	WP3, Hazard and Impacts Method Development	
WP Lead /Deliverable beneficiary	GEUS/BRGM	
Deliverable status		
Submitted (Author(s))	30/09/2021	Hideo Aochi
Reviewed/Verified(WP leader)	30/09/2021	M. Delatre [BRGM], T. Larsen (GEUS)
Approved (Project leader)	14/10/2021	Hans Doornenbal [TNO]

TABLE OF CONTENTS

1 INTRODUCTION

1.1 Document Background and Scope

This document presents the HIKE WP3 final report after mid-term report. The document contains a description of the case study methodologies, case study settings, the works done and the perspectives. This document also focusses on expected interaction with the European Fault database (FDB) and cross cutting relations between case studies. It is the objective to give an in-depth description of the individual case study, and to show the way forward beyond the current knowledge.

1.2 Abbreviations

HIKE	= Project ”Hazards and Impacts Knowledge Europe”
GIP	= Project ”Geo-Information Platform”
EGS	= EuroGeoSurveys organization
GEEG	= Geo-Energy Expert Group (EGS)
EOEG	= Earth Observation Expert Group (EGS)
MREG	= Mineral Resources Expert Group (EGS)
WREG	= Water Resources Expert Group (EGS)
SIEG	= Spatial Information Expert Group (EGS)
EC	= European Commission
MS	= Member States
NGO	= Non-Governmental Organization
EGDI	= European Geo Data Information Platform
DMP	= Data Management Plan
PIP	= Project Implementation Plan
PMB	= Project Management Board (project lead + work package leads)
PA	= Project Assembly
PL	= Project Lead
WPL	= Work Package Lead
TL	= Task Lead
CDE	= Communication, Dissemination and Exploitation (plan)
FDB	= Fault database
HIDB	= Hazard and Impacts database
SHARE	= Project ”Seismic Hazards Research Europe”
EPOS	= Project ”European Plate Observing System”
MICA	= Project ”Mineral Intelligence Capacity Analysis”
DOI	= Digital Object Identifier
GSO	= Geological Survey Organization
INSPIRE	= Infrastructure for Spatial Information in Europe
GEOSCIML	= data model and data transfer standard for geological data
SI	= International System of Units

1.3 HIKE WP3 contributors

#	Participant Legal Name	Institution	Country
1	Nederlandse Organisatie voor Toegepast Natuurwetenschappelijk Onderzoek TNO	TNO (coordinator)	Netherlands
2	Albanian Geological Survey	AGS	Albania
3	Geologische Bundesanstalt	GBA	Austria
4	Royal Belgian Institute of Natural Sciences – Geological Survey of Belgium	RBINS-GSB	Belgium
5	Geological Survey of Denmark and Greenland	GEUS	Denmark
6	Bureau de Recherches Géologiques et Minières	BRGM	France
7	Bundesanstalt für Geowissenschaften und Rohstoffe	BGR	Germany
8	Landesamt für Bergbau, Geologie und Rohstoffe Brandenburg	LBGR	Germany
9	Landesamt für Geologie und Bergwesen Sachsen-Anhalt	LAGB	Germany
10	Bayerisches Landesamt für Umwelt	LfU	Germany
11	Islenskar orkurannsoknir - Iceland GeoSurvey	ISOR	Iceland
12	Istituto Superiore per la Protezione e la Ricerca Ambientale	ISPRA	Italy
13	Servizio Geologico, Sismico e dei Suoli della Regione Emilia-Romagna	SGSS	Italy
14	Agenzia Regionale per la Protezione Ambientale del Piemonte	ARPAP	Italy
15	Lietuvos Geologijos Tarnyba prie Aplinkos Ministerijos	LGT	Lithuania
16	Państwowy Instytut Geologiczny – Państwowy Instytut Badawczy	PIG-PIB	Poland
17	Laboratório Nacional de Energia e Geologia	LNEG	Portugal
18	Geološki zavod Slovenije	GeoZS	Slovenia
19	State Research and Development Enterprise State Information Geological Fund of Ukraine	GEOINFORM	Ukraine

2 HIKE WP3 CASE STUDY AMBITIONS AND EXPECTED IMPACTS

2.1 The case study concept

HIKE WP3 aimed to develop and test novel methodologies building on top of results from previous projects and research. The work is expected to advance current state-of-the-art knowledge across different energy exploitation scenarios and various geological settings. The final goal is to improve hazard and impact assessments and provide the basis for better standardization of these evaluations across Europe.

The Task 4 of WP3 targeted the seismicity in Lacq-Rousse area, southwestern France, where the gas extractions had been held and a CO2-injection experiment was carried out in the reservoirs. The main concern of the area's seismicity is to distinguish if an earthquake occurred within a reservoir or outside. The former is considered as induced seismicity. The latter is regarded as a triggering event if mechanical impact of the reservoir is likely, or a natural one if the tectonic involvement is considered major. For judging this, the known fault structure plays an important role. The precise location of the earthquakes is always important; however, the limit in resolution makes it difficult to identify an individual fault as origin of the events. On the other hand, the focal mechanism brings information on the stress field behind the earthquake. It is essential to understand if the stress field is consistent with the known fault structure, with the mechanical understanding of reservoir behavior and/or the tectonic system of the area.

2.2 Summary of case study technologies

This reports on the following specific topic:

- Assessment of seismicity and safety in storage, Lacq Rousse, France case study

For this purpose, we study mainly the focal mechanism inversion using full-wave forms for the recent moderate earthquakes (Magnitude of about 4). We also use statistical analysis of the seismicity during the CO2 injection experiment to demonstrate how can we assess the evolution of the seismicity.

3 OBJECTIVES OF THE CASE STUDY ON LACQ-ROUSSE

The Lacq-Rousse (Southwestern France) area is a depleted gas field, whose commercial exploitations ended in 2013. CO2-injection and storage experiment was carried out in 2010-2013 (51 kton in total) (Thibault et al., 2014). Although the CO2 injection did not induce any significant earthquakes in the area, a few felt earthquakes of magnitude up to 4.5 has been observed since 2014 (Aochi & Burnol, 2018). It is an important task to distinguish if the earthquakes are induced, triggered or natural one. The seismicity in the area is monitored by public observational networks. The publicly accessible catalog is provided by Bureau Central Sismologique Français (BCSF) and Réseau National de Surveillance Sismique (Rénass) (http://www.franceseisme.fr/sismicite.html, last accessed as of the 31st may 2021). A few earthquakes of magnitude 3.5-4.0 are known in the area. We observe that the seismicity is detected down to magnitude 1.5 in the area (Figure 1). Although the precise mapping of the seismicity (many earthquakes) generally allows identifying the activated fault structures, a few kilometers of errors remain due to the sparse station distributions and the fact that the earthquakes occurred isolated with no obvious aftershocks. A single earthquake can provide useful information with moment tensor solutions to verify the coherency of the mechanism with the known fault structure and tectonic settings. Thus, the objectives of this case study are (1) archiving the available catalogs and (2) performing the moment tensor inversions of moderate earthquakes to complete our knowledge in the area.

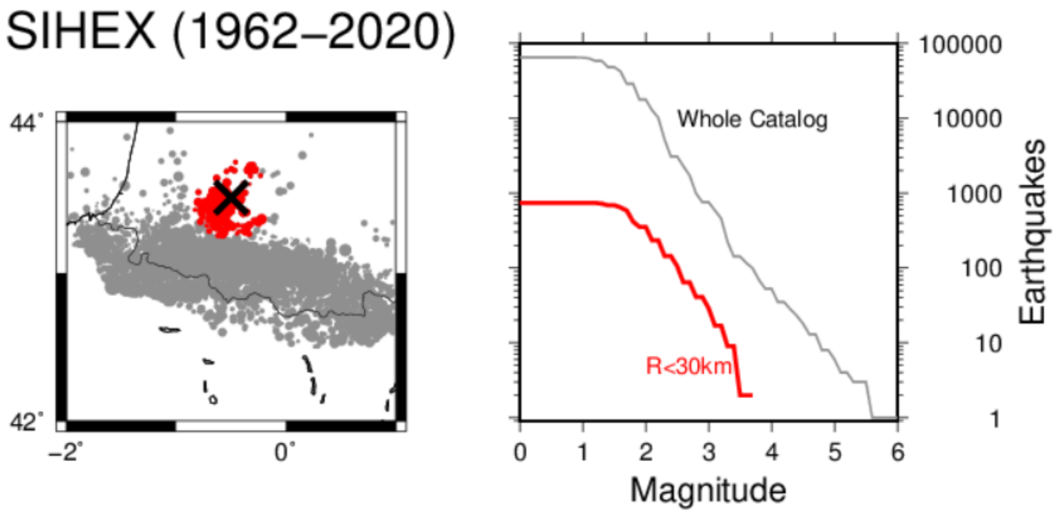

Figure 1 : Map of the seismicity in the Pyrenees, southwestern France from the SIHEX catalogue. A point of interest is chosen for (43.5°N, 0.5°W) and the seismicity within a radius of 30 km is colored by red. The magnitude-frequency relations are shown on the right panel both for the whole catalog (whole France) and the selected area.

4 SUMMARY/ABSTRACT

The Lacq-Rousse gas field is significantly relaxed within the reservoirs regardless of the CO_2 injection experiments as of 2013. Felt earthquakes occurred in the upper crust above the reservoirs in 2013, 2016 and 2017. These are considered to have released the residual stress of the crust due to the compaction of the reservoirs. The obtained mechanisms are qualitatively consistent with the known fractures systems, briefly NWW-SEE running faults and the estimated Coulomb stress change due to the compaction of the reservoir. However, it is difficult to identify a particular fault to each earthquake, because of the limit of location precision, the embedded structure for moderate earthquakes (Mw3.25, Mw3.9 and Mw3.21, respectively) and the isolated occurrence with no aftershocks. On the other hand, the recent 2020/06/20 Mw3.5 earthquake is a strike-slip faulting mechanism at a depth deeper than the reservoir. This is considered instead as a natural earthquake, but no particular fault is identified. Our study provides an increment in the understanding of the current status of the reservoir and the surrounding seismicity.

5 KEYWORDS

Pyrenees, Lacq-Rousse, CO2 injection, depleted reservoir, focal mechanism.

6 GEOLOGICAL SETTING

The Lacq-Rousse gas field is located approximately at 5 km depth. The geological structure is aligned parallel to the Pyrenees mountains running approximately in the NWW-SEE direction (Figures 2 and 3). The cross-sections confirm the folded structure perpendicular to the mountain front, represented with many thrust faults (e.g. Beteau et al., 2006; Bardainne et al., 2008; Thibeau et al., 2013). Although some main structures (e.g. North Pyrenean frontal thrust) related to the tectonics reach the ground surface, many embedded faults covered by sedimental layers are associated around the reservoir depth, only revealed from high-resolution seismic tomography. After Bardainne et al. (2008), we reconstruct the 3D model of the area, approximately covering 20 km x 20 km x 10 km for the 3D wave propagation in our study. The model reflects the structural difference with respect to the South Lacq fault. The other small faults (fractures) are not identified in this model. Later we use this model for 3D seismic wave propagation simulations as shown in Figure 4.

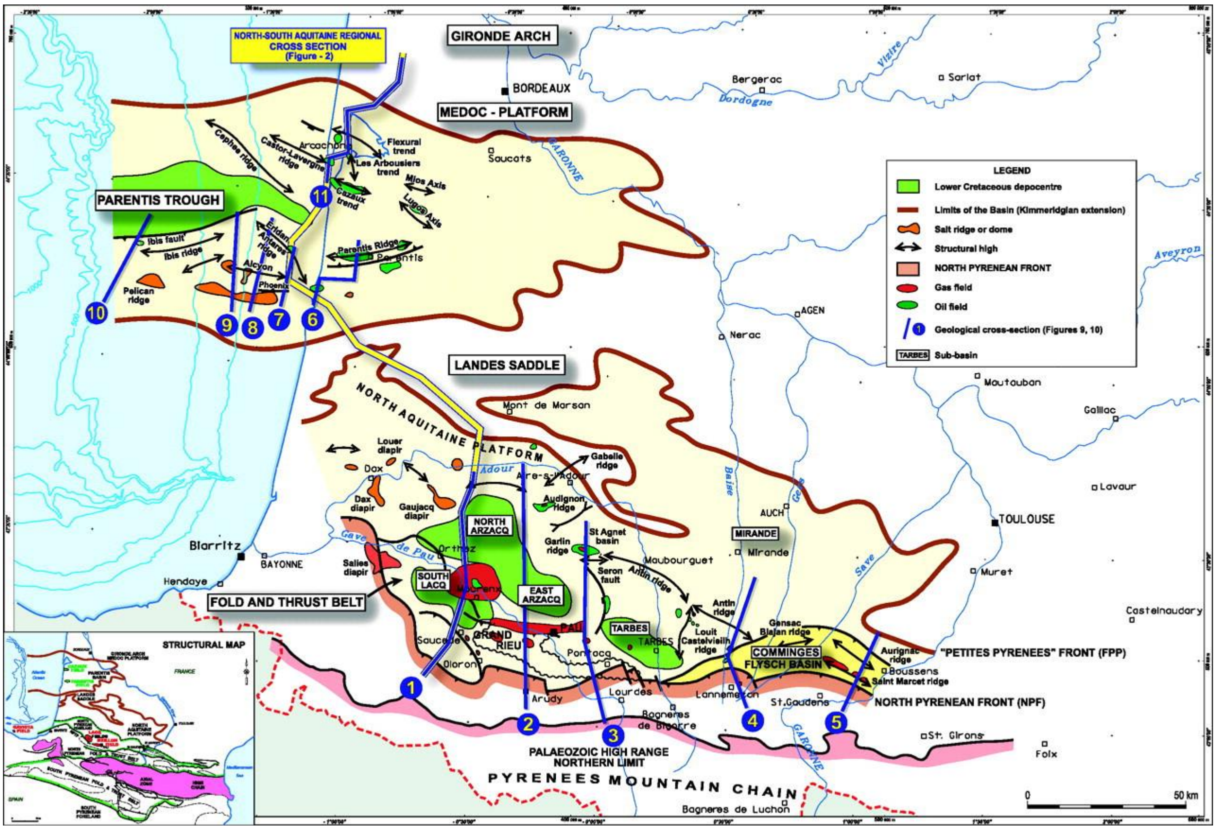

Figure 2: Illustration of the Aquitaine Basin, southwestern France (Biteau et al., 2006)

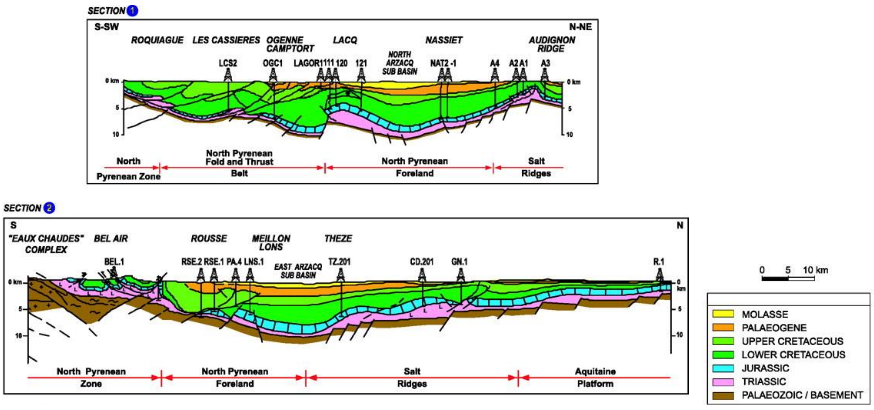

Figure 3 : Cross-sections (Biteau et al., 2006).

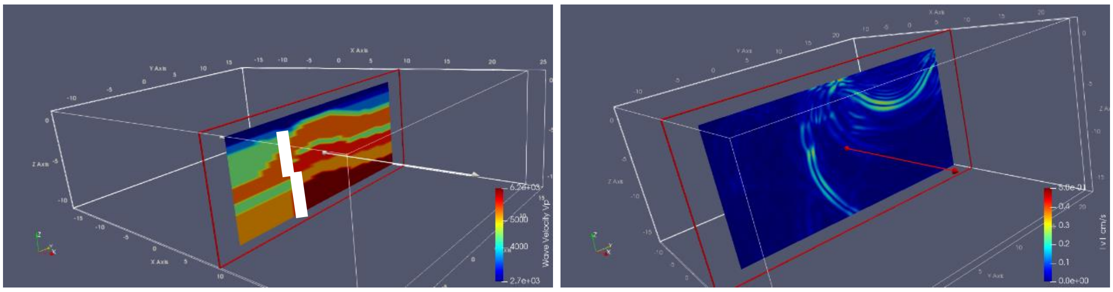

Figure 4 : Left : NS cross-section of 3D structure around Lacq area reconstructed after Bardainne et al. (2008) and the other literatures. Right: An example of 3D wave propagation simulation of the 2016 earthquake.

7 CASE STUDY ENERGY EXPLOITATION/STORAGE

The induced seismicity due to the exploitation is known since 1969 (Wittlinger, 1980; Volant and Grasso, 1994). The pressure at Lacq is reduced from 65 MPa at the end of 1950's to 10 MPa in 1990. The maximum magnitude ML4.2 was detected in 1978 and the subsidence was measured to 2.5 cm between 1867-1979. All these data in old literatures were collected and achieved by ourselves for further studies. After the end of exploitations in 2013, the seismicity in the area continues with the ML4.0 2016/04/25 earthquake (Aochi and Burnol, 2018). In parallel, a CO2 injection and storage experiment has been carried out in one of the near-by reservoirs at Rousse between 2010 and 2013. This was monitored well by a dense borehole network. The injected volume and the increase of the pressure remains small, and the observed seismicity was localized only around the injection well without activating any fault (fracture) at distance. The microseismicity becomes quiet back to the level of the background seismicity level quickly (Maury et al., 2019). This case is considered as a well-controlled case of injection-related seismicity.

The purpose of our task in this project is to achieve the data from the literature for further usage. We summarize it in the following.
Pore pressure change of the Lacq reservoir from 1960 to 2000. (

- Figure 5)
- Plotting recent earthquakes (2013, 2016, 2017) which we have analyzed on the seismicity during the exploitation (1974-1983). (*Figure 6*)
- The seismicity evolution in the early days (1969 to 1979). (*Figure 7*)
- Vertical displacement across Lacq reservoir. (*Figure 8*)
- Pore pressure change of the Rousse reservoir from 1974 to 2013. (*Figure 9*)
- The seismicity evolution during the CO2 injection experiment from 2010 to 2013. (*Figure 10*)

We remark that the early day's data were published on paper only and they are not always coherent with each other. For example, in the time scale (

Figure 5) or in the positions (*Figure 6*). However, globally we could construct the understandable, exploitable data sets. The pressure decreases both at Lacq and Rousse is significant from 60 MPa to 5 MPa, and 40 MPa to 5 MPa, respectively, for as long as we can know. In contrast, the increase of CO2 injection from 2010 to 2013 remains small, far from the early day's reservoir state.

In particular, Maury et al. (2019) analyzed the Rousse data (*Figure 9* and *Figure 10*) from the point of view of statistical seismology, by applying the non-stationary Epidemic-Type Aftershock Sequence (ETAS) model. The ETAS model (Ogata, 1988) describes the seismicity rate $\lambda(t)$ (daily earthquake of magnitude equal to and larger than M_c) as background seismicity rate μ due to any external forcing and the earthquake interaction in form of the summation from the past earthquakes:

$$\lambda(t) = \mu \quad + \sum_i K e^{\alpha(M_i - M_c)} \frac{1}{(t + c - t_i)^p}$$

where five basic parameters (μ, K, α, c, p) are included. The two principal parameters are μ as background seismicity rate and K as triggering seismicity rate. α indicates the magnitude dependency of the triggering effect ($\alpha \ll 1$ indicates no dependency of magnitude, namely the seismicity is purely point-process). The parameters (c, p) are those in the modified Omori's aftershock law (often $c \ll 1$, and $p \sim 1$). For the seismicity driven by tectonics, the background seismicity rate μ is usually considered constant, invariant with time. However, in the context of induced seismicity, one has to consider that μ is variable with time according to the injection operation (well pressure, injected fluid volume), reflecting the mechanical fact that increase of pore pressure makes the rupture easy. Maury et al. (2019) tested two formulations

$$\mu_{ind} = \begin{cases} c_f f(t) \text{ during the injection} \\ \mu_0 + Be^{-\gamma t} \text{ for post-injection} \end{cases}$$

where $f(t)$ is known injection rate or well pressure change and the other parameters (c_f, μ_0, B, γ) are constant such that μ_{ind} is continuous (*Figure 11*). Although the first equation is written uniquely, its coefficient c_f may have some variation according to each injection phase, as we usually observe in the deep geothermal site (e.g. Maury & Aochi, 2021). For this site, we do not have raw data of injections, and the curves are approximative after Thibault et al. (2013) so that it is difficult to discuss quantitatively the results. On the other hand, coefficient γ represents the relaxation of the seismicity after the shut-in, and is found $\gamma = 0.048\ (1/day)$. Namely the seismicity reduces by 1/20 after 60 days.

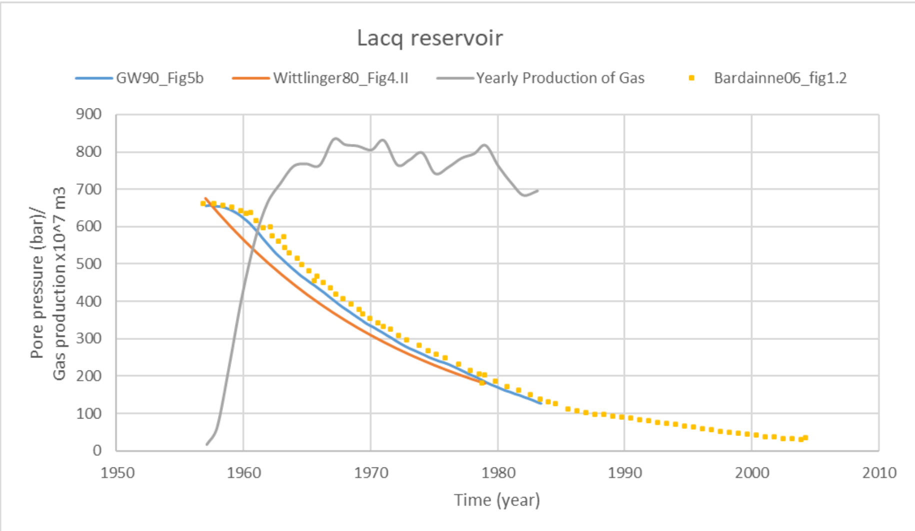

Figure 5 : Pore pressure change of the Lacq reservoir and yearly gas production. The data from Wittlinger (1980), GW90 (Grasso and Wittlinger, 1990) and Bardainne et al. (2008).

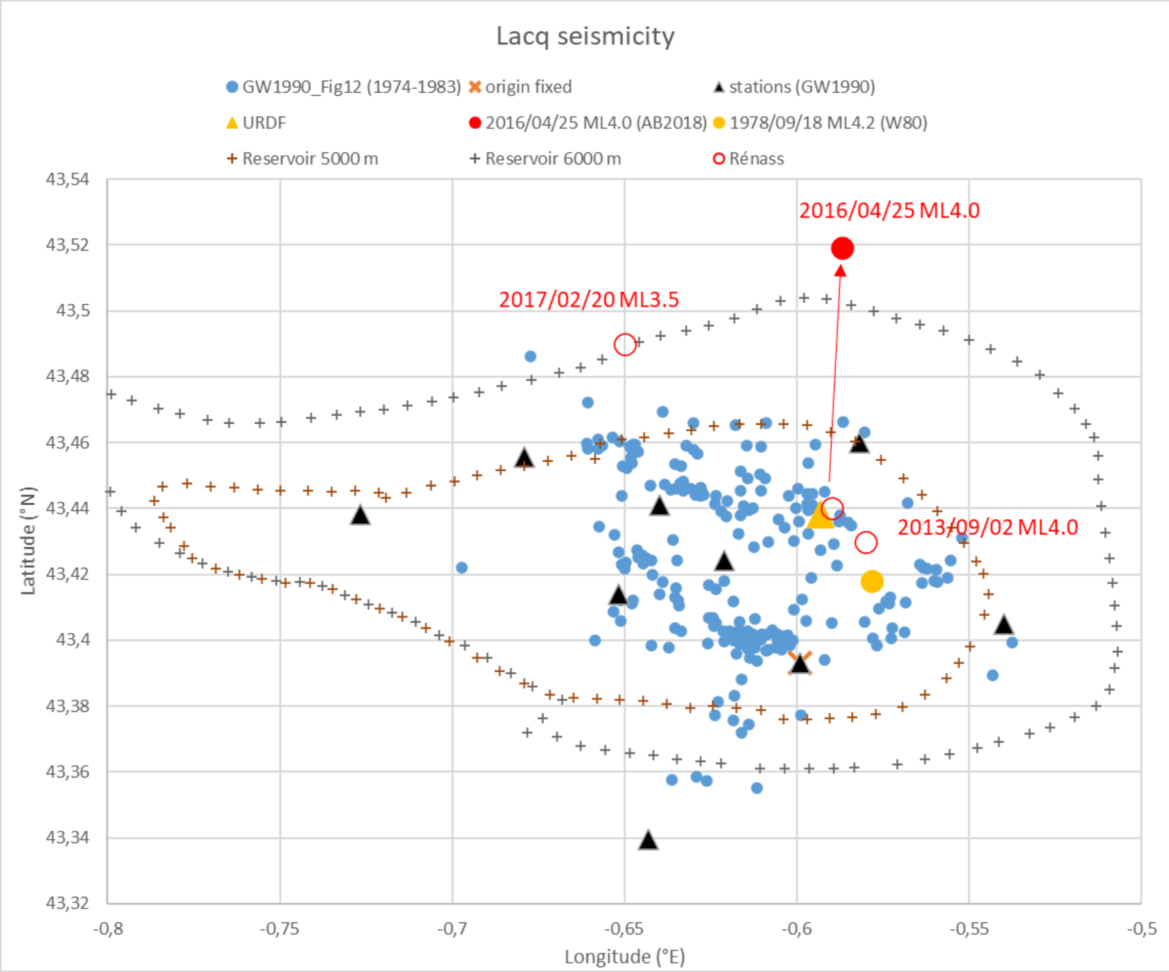

Figure 6 : Map from the compiled data around Lacq reservoir. The reservoir depths (Bardainne et al., 2008). The seismicity during the exploitation between 1974-1983 (Grasso and Wittlinger, 1990; GW1990) with the stations at that day (blue triangle). The three recent earthquakes are shown by open circle (Rénass) and the epicenter location of the 2016/04/25 event by solid circle (Aochi and Burnol; 2018).

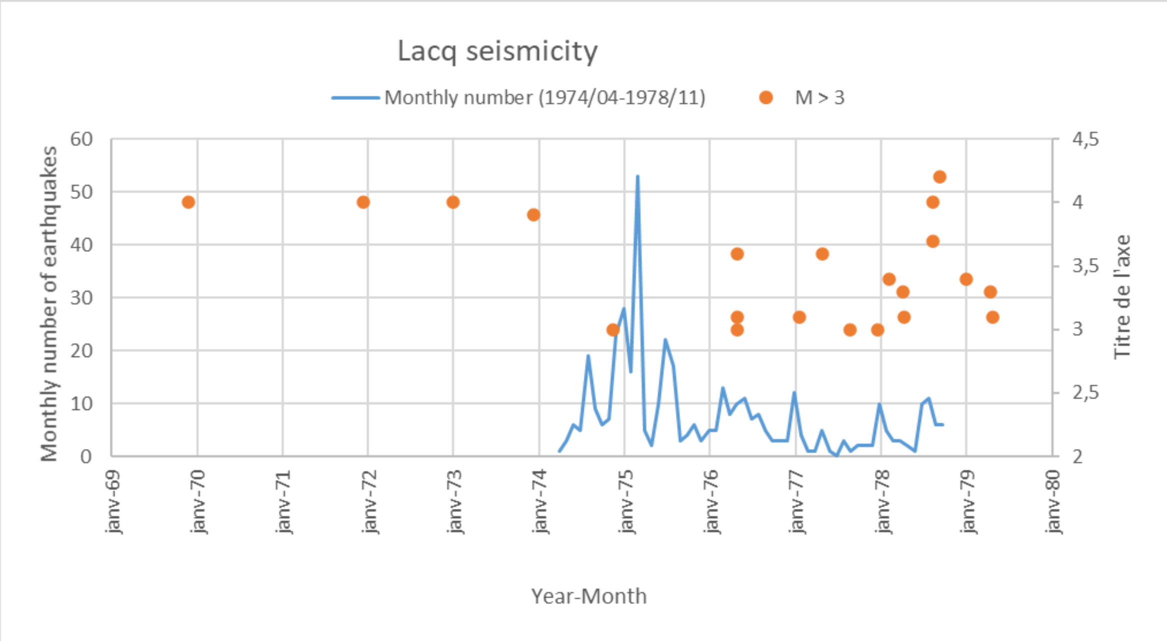

Figure 7 : Seismicity evolution from 1969 to 1979 (Wittlinger, 1980).

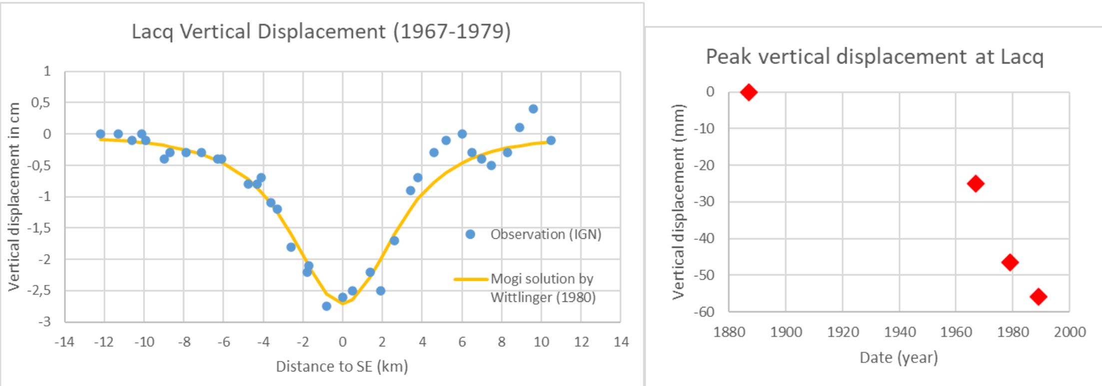

Figure 8 : Vertical deformation across Lacq reservoir. Left: the profile from NW to SE during 1967 and 1979 (after Wittlinger, 1980). The peak vertical displacement since 1987 to 1989 after Segall et al. (1994).

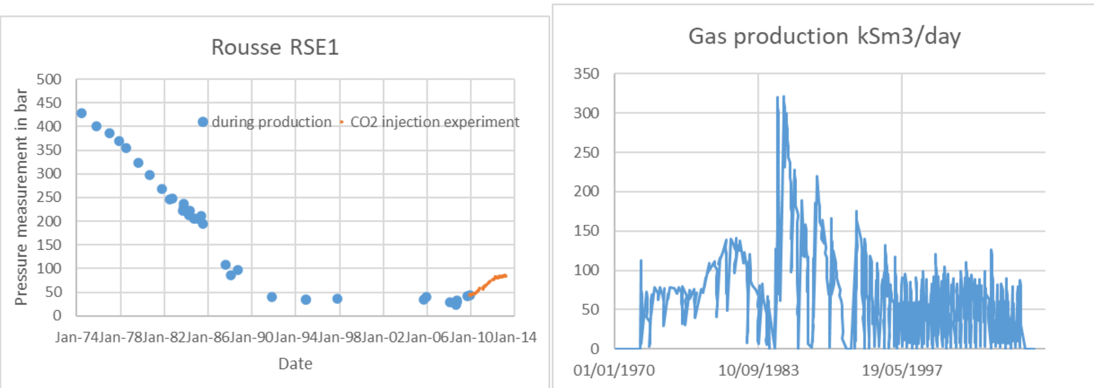

Figure 9 : Pore pressure change at Rousse reservoir from 1974 to 2013 and the gas production from 1970 to 2009 (Thibaut et al., 2013).

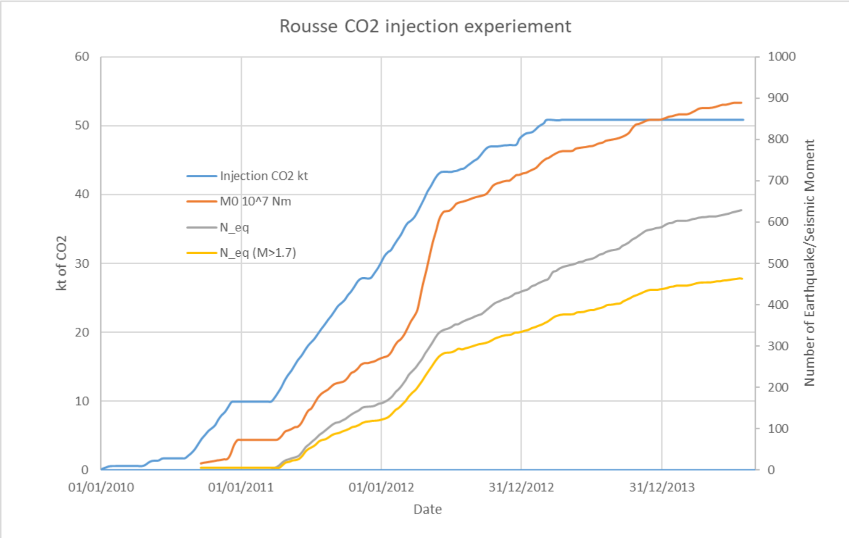

Figure 10 : Seismicity evolution and CO2 injection during 2010 and 2013 at Rousse (Payre et al., 2014).

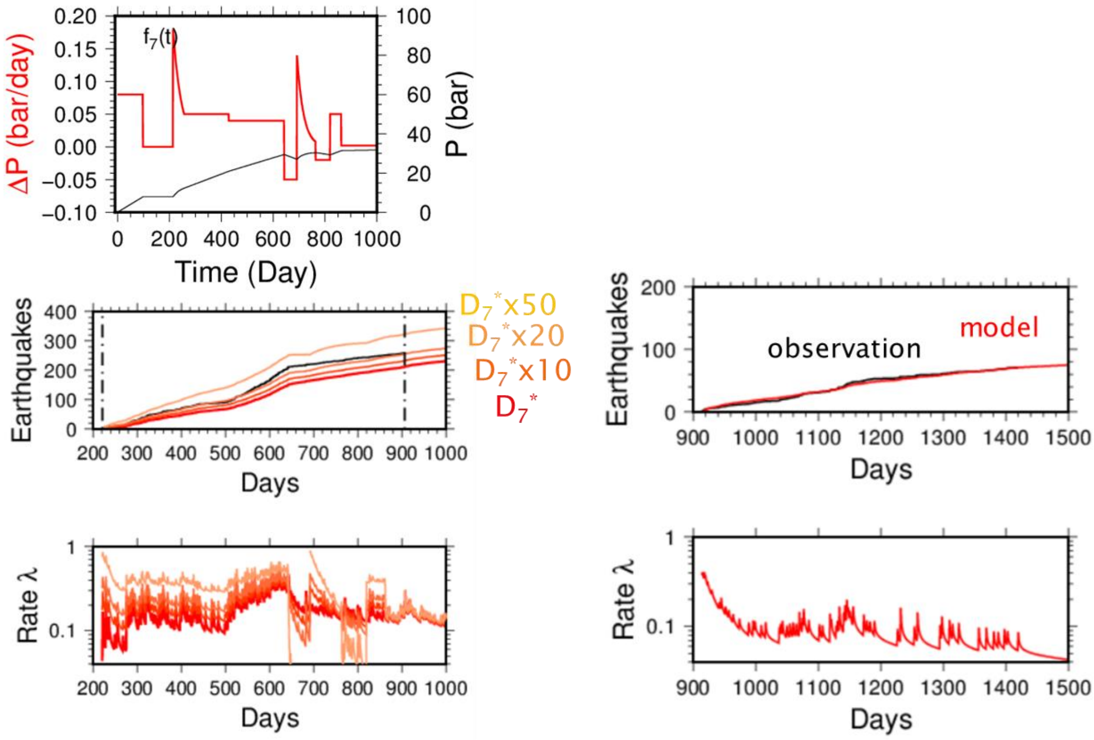

Figure 11 : ETAS analyses on the 2010-2013 Rousse experiment after Maury et al. (2019), for the period of injection at left panels and post-injection at right hand side. For the period of injection, pore pressure change is assumend to be a basic function f(t) and four different parameters with respect to the reference value $c_f = D_7^*$ to show the sensibility. The injection information is not based on raw data, but approximative after Thibault et al. (2013). For the post-injection, a set of the parameters fits well the observation. The synthetic seismicity rate λ is shown at bottom.

8 METHODOLOGY/ ANALYSIS/ UNCERTAINTY EVALUATION/ DISCUSSION

We aimed to analyse seismologically the important recent earthquakes. We used the regional, public seismic networks to obtain the focal mechanism and refine the seismic location (focal depth). The data are achieved and available in the framework of EPOS-ORFEUS (http://orfeus-eu.org/webdc3/, last accessed on the 18th June 2021). The inversion process is based on the Aochi and Burnol (2018), in which the seismograms are filtered in a limited band of frequency and the Genetic Algorithm is deployed for obtaining the mechanism (strike, dip, rake) and the magnitude. We fixed the epicenter position provided by Rénass (https://renass.unistra.fr/fr/zones/) and vary the focal depths to seek a better fit of the seismograms. The synthetic seismograms are calculated in a 1D layered model, as we only use the low frequency (10 seconds or longer). Forward modeling of seismic wave propagations is carried out in a locally available 3D mode using a finite difference method (Aochi et al., 2014).

The following table summarizes the earthquakes we have anlaysed. In particular, we focused on the 2020 event, which occurred in the vicinity of the reservoir and thus was questioned whether this is a tectonic or induced event (Figure 12). We demonstrate our inversion process for this earthquake (Figure 13). Five stations are available in the vicinity. However, after some trials, we do not use the nearest station URDF and the northernmost station TERF. The URDF, located too close to the earthquake, becomes dominant in the inversion process, however, the waveforms are significantly influenced by the precise location of the earthquakes, while the regional catalog may have un certainty of a few km in this area (e.g. Aochi and Burnol, 2018). The TERF is located far from the Pyreneans mountains and the used 1D model may not be suitable as the wave fitting has some phase shift. Thus finally, the three other stations are adopted. The fitting for the three stations is good enough to provide a stable mechanism (strike-slip faulting). On the other hand, the convergence of the fitting with respect to different focal depths is not significant. As the focal depth is estimated deep, the difference is not so visible as the deeper structure is homogeneous. Nevertheless, this analysis confirms that the earthquake should have occurred at depth, beneath the reservoir depth. The strike-slip faulting is also different from the known mechanism (normal faulting above the reservoir) so that we conclude that this earthquake was a tectonic event.

The uncertainty of the analysis mainly comes from the reliability of the adopted structure for a given frequency range and the available station coverage. As a demonstration, we show, in Figure 14, the comparison of the particle ground motions at URDF for the 2020/06/03 event. If the given epicenter position is correct, the 3D structure better reproduces the beginning of the particle motion (the arrival of P-wave). As the resolution of 3D model is still limited, the precision of the earthquake location is so as well. We will need further acquisition of data to verify the implemented model and the simulation results.

Events	Location	Magnitude	Mechanism (strike,dip,rake)	Comment
2013/09/02 ML4.0	-0.58°E, 43.43°N, 5 km	Mw3.25	(263.56°, 35.4, -90.3°)	Loc. Rénass

2016/04/25 ML4.0	-0.5869°E, 43.5191°N, 4 km depth	Mw3.9	(66.3°,32.0°,-114.6°)	Relocalised.
2017/02/20 ML3.5	-0.65°E, 43.49°N, 6 km	Mw3.21	(7.17, 38.22°, -170.88°)	Loc. Rénass. Poor convergence.
2020/06/03 ML3.1	-0.551°E, 43.439°N, 8.5 km	Mw3.6	(196.8°, 85.7°, 184.1°)	Loc Rénass. Depth convergence poor.

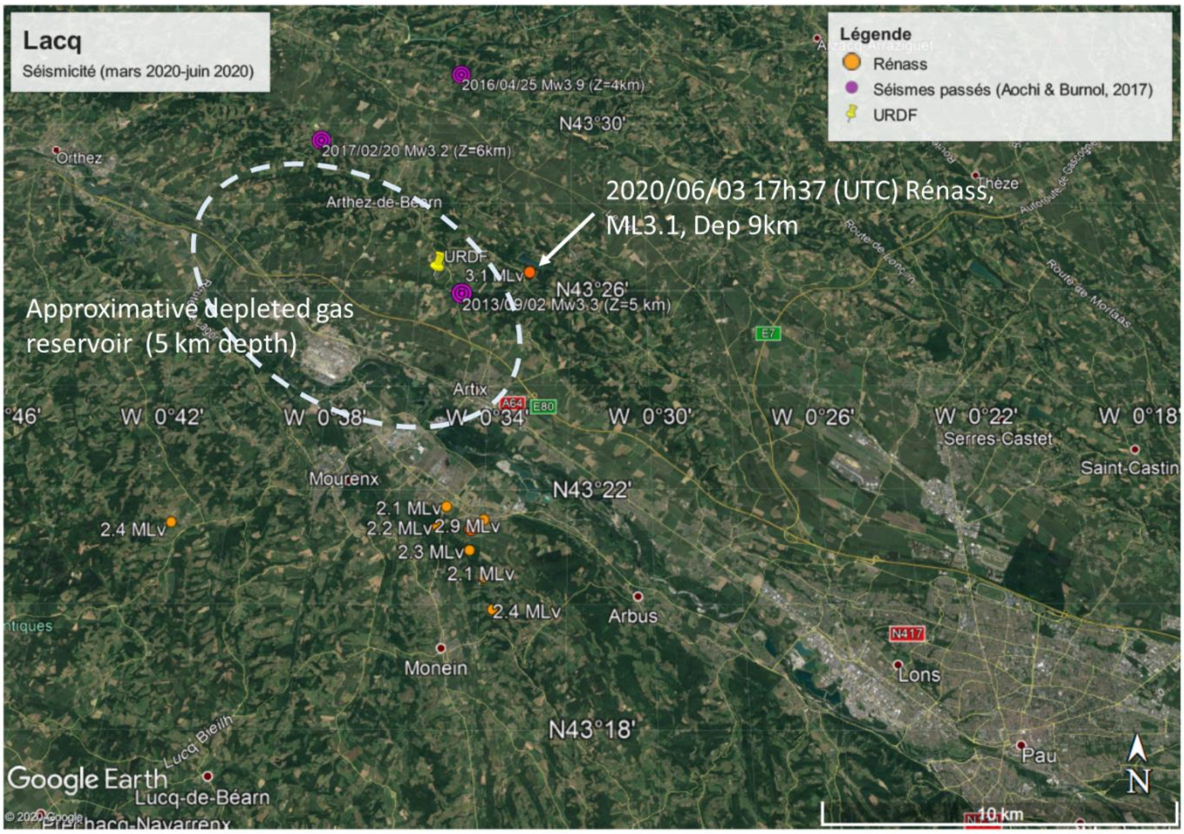

Figure 12 : Map of around the Lacq reservoir and the seismicity. The approximative extension of the reservoir at 5km depth is illustrated by an oval. The 2020/06/03 ML3.1 earthquake occurred in the eastern edge of the reservoir. The three other earthquakes (2013, 2016, and 2017) are plotted as purple circles. The seismicity in the area (March 2020 to June 2020) are shown in orange plots which are located in the southernmost structure boundary (see 3D model). The seismic station URDF is shown by yellow pin located above the reservoir.

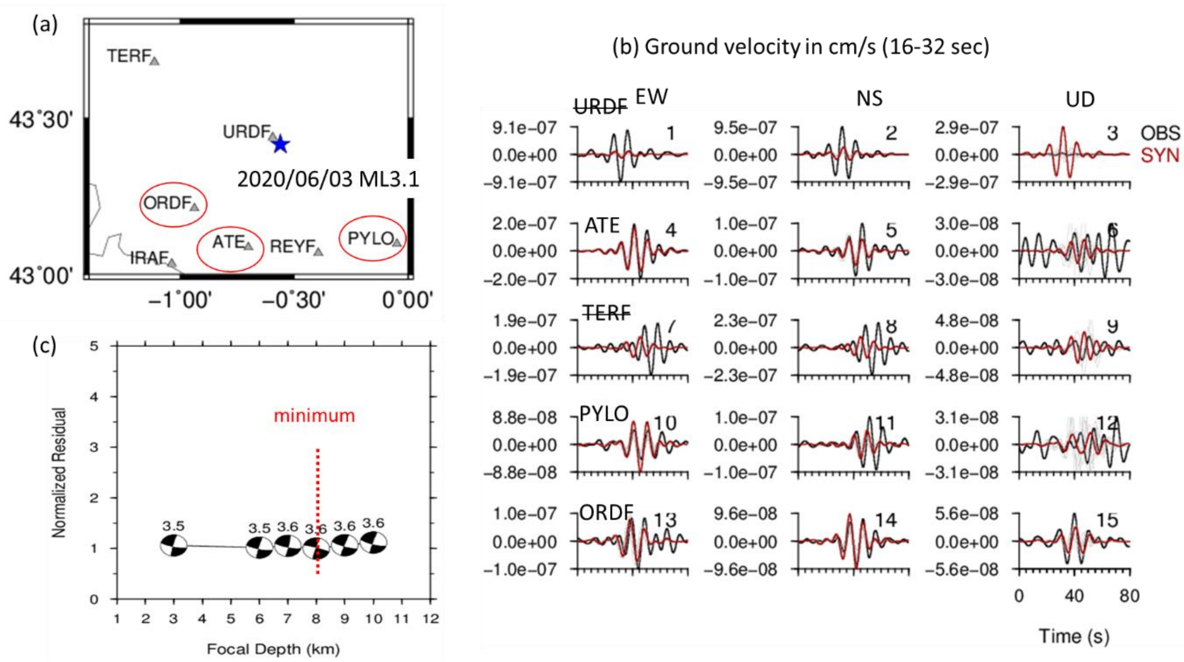

Figure 13 : The analysis for the 2020/06/03 event. (a) Map of the stations and the epicenter. Three stations are used for the inversions. (b) Fitting of the synthetic seismograms to the observations. The forward comparisons are also shown for URDF and TERF, which are not included for the inversion. (c) The convergence of the fitting with respect to the different focal depths. The obtained mechanism and magnitude are shown. The best fitting is found for the focal depth of 8 km.

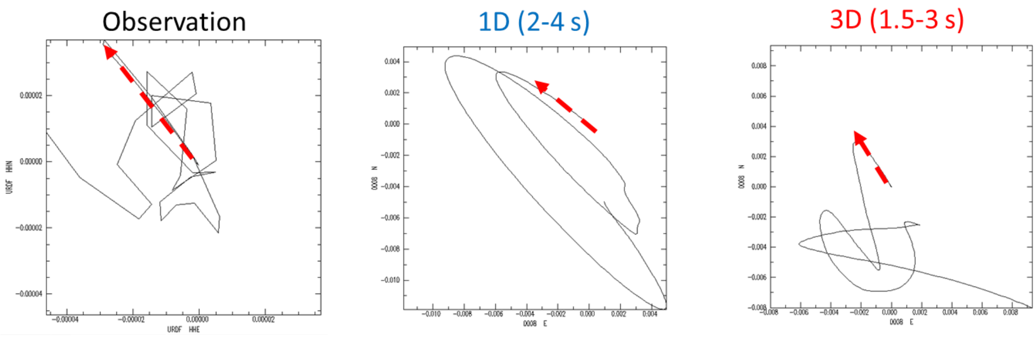

Figure 14 : Comparison of the particle motion (horizontal plane) for the 2020/06/03 earthquake. From left to right, the observation at URDF and the synthetics in 1D and 3D structures, respectively.

9 POTENTIAL IMPACT

The seismological assessment of the reservoir for a long term is important to assure the security and potential usage. After the end of exploitation in 2013, it is inferred that the residual stress due to the reservoir's compaction plays an imporatnt role for the recent felt earthquakes, while the infuence of the CO2 injection experiment has disappered very quicky according to the statistical analysis. This infers that the change of stress field due to the exploitation is dominent in the area. It is crucial to estimate how long it takes to relax the residual stress for the regional seismic hazard assessment. It is also important to follow up on the seismicity and reservoir state, not only for the current security but also for the potential (re)use of the reservoir such as underground gas storage or CO2 storage.

10 IMPORTANCE OF FAULT DATABASE TO SEISMOLOGICAL METHODOLOGY

Precising mapping of the seismicity is essential to understand the fault system of the area. However it is not always possible, because the precise location of the earthquakes requires a dense seismic network at the surface and, if possibe, at depth. The studied area does not benefit from such dense network. Instead, we studied the focal mechanism of large earthquakes (magnitude 3 to 4), as summarized in Figure 15. The focal mechanism soution reflects the stress field behind so that this helps to interpret the area's geodynamical system with known faults. In the case of the reservoir, most faults are embeded, which are not mapped on the surface geology map and may not be active from the point of view of tectonics. The existence of the embeded faults are interpreted through geophysical exploitation such as reflecting seismology. Due to the limit of the structure resolution and earthquake locations at depth, it is difficult to identify any explicit fault to each earthquake. Thus, it becomes important to study the focal mechanism to check if the stress field is consisetent with the known fault structure and the structure geology.

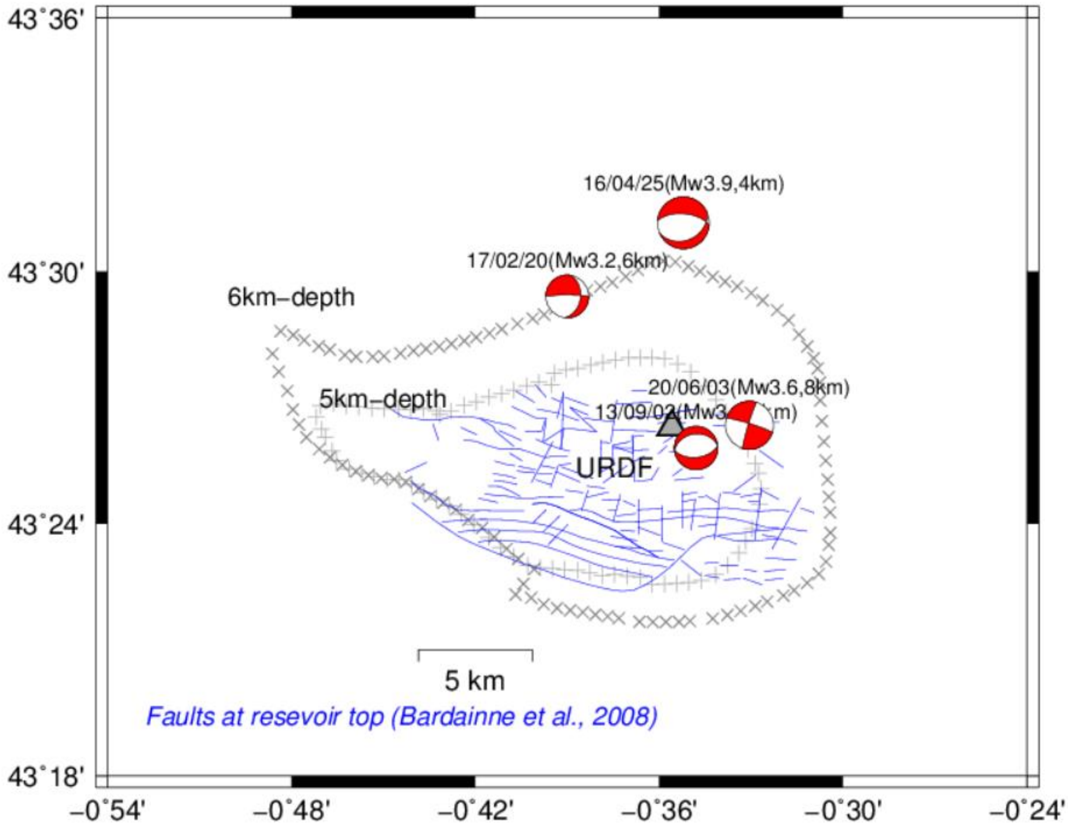

Figure 15: Summary of the analysis of the four recent earthquakes, superposed on reservoir and fault map.

11 CROSS-CUTTING RELATIONS BETWEEN CASE STUDIES

The case studies apply different methodologies to the study of the potential hazards and impacts across several different kinds of energy exploitation. Methodologically, this task 4 of WP3 is closely related to T3.1. In addition to the energy exploitation type/hazard methodology cross-cutting relations, two overarching common themes will be explored: 1) How the different methodologies deal with uncertainties in different situation, and 2) how to improve the input to guidelines made by authorities.

11.1 Cross-cutting: uncertainty estimates

In T3.4 **Seismicity and safety in storage** the questions related to uncertainty are similar to those in T3.1. Two different setups will be studied; Evaluation of many small earthquakes on a dense, local network vs fewer, larger events on a distant, sparse network. Moderate earthquakes of magnitude of about 4 in Lacq-Rousse area occurs as individual events with no aftershocks. They were not related to any known faults, but the focal mechanisms are consistent with the area's fault structure and stress field behind. In the focal mechanism analysis, we have to fix the epicenter location. Thus, the precise location of earthquakes is very important. We studied the uncertainty of the focal depths for all the events. From the limitation of current resolution, there remains an uncertainty of about 1 km vertically. However, this was enough to distinguish if the event is at the depth of reservoir or below/above it, namely if the earthquake is induced event or natural. When it comes to the solution in a 1D layered model vs a 3D heterogeneous model, the current configuration (only 1 station available in the near field) does not allow to validate the model. At least a few stations covering the area will be necessary in the future.

11.2 Cross-cutting: Scientific basis for guidelines to authorities

A common, cross-cutting goal for all of the case studies is the desire to provide improved input to authorities writing guidelines for the safe energy exploitation of the subsurface. From the results of this task T3.4, it is important to know the spatial-temporal expansion of the influence due to the operation in the reservoir. The event of 2016 (10 km away from the deepest point of the reservoir and a few kilometers from the edge of the inferred reservoir) is consistent with the change of stress field led by the reservoir compaction. On the other hand, the event of 2020 is even closer to the reservoir, but it is found that the focal depth is deeper than the reservoir and the mechanism is different from the reservoir-induced earthquake and we conclude that this was a tectonic event (this report). These facts imply the need to monitor the seismicity not only within the reservoir and during the operation, but also in a larger area for a longer period. We will also need a continuous, systematic study on the seismicity to monitor any possible evolution and archive the results as dataset for further utilization, because we need to compare an event with the past seismicity.

As seen in the induced seismicity in the geothermal sites such as Pohang (South Korea; Korean Government Commission, 2019) and Strasbourg (France, Schmittbuhl et al., 2021), the seismological analyses provide the scientific base for debating the implication of the operation in the seismicity. What we have learned is that we need the transparency of the dataset and knowledge and the guidelines should not be changed without scientific understanding behind.

12 BEST PRACTICE WITHIN THE FIELD OF SEISMOLOGICAL METHODOLOGY

We always need to continue monitoring the area's seismicity of interest. It is essential to have a dense network, but one can still work with the available data even if the data is not abundant. As demonstrated in this report, it is important to use the full waveforms. We used a limited frequency band only, and it is expected that the analysis on different frequencies may bring more complementary information. The data transparency is consistent with the requirement in the current research activities. The new trends such as citizen seismology (portable seismograms by habitants), fiber-optic seismograph, and machine-learning technique to detect better the seismic events (e.g. Ross et al. 2020) will complete our knowledge by the traditional heavily instrumented seismological methodology. Figure 16 shows a successful example of machine learning technique revealing the detailed structure of faults and seismicity evolution in the Southern California (Ross et al., 2020). However, this is an ideal case of natural seismicity with many events in an area of high seismic activity. Alternatively, it is important to detect aseismic slip and deformation to monitor the reservoir state and fluid movement.

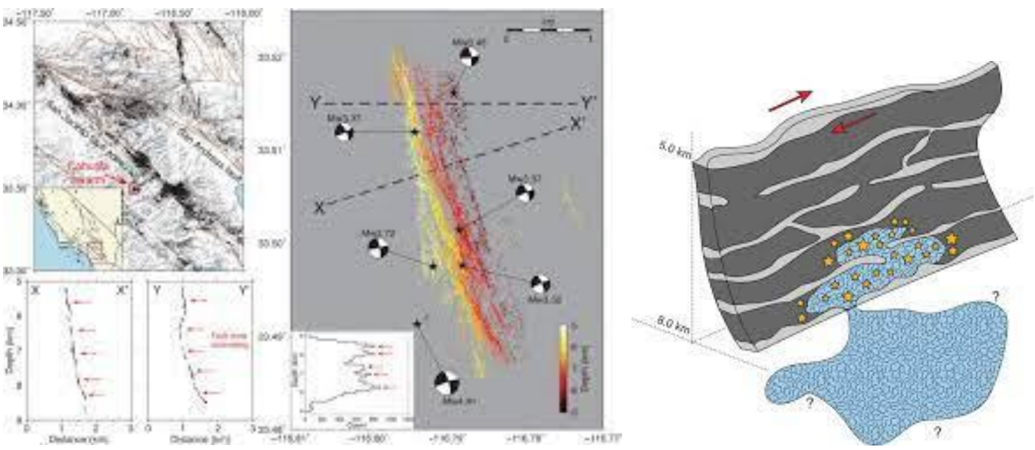

Figure 16: Faults responsible for earthquakes are idealized into two dimensions, despite fault zones being complicated, three-dimensional structures. Ross et al. 2020 used machine learning to find 22,000 seismic events near Cahuilla, California, during a seismic swarm. They used the locations and sizes of these events to show how the complex structure of the fault (left panel) interacted with natural fluid injections from below (right). The authors' methods highlight the complexities of one fault and suggest a way to characterize other faults around the world.

One interesting aspect would be a statistical analysis of the seismicity related to the injection/extraction process. This was not the purpose of this task but this is overviewed briefly in Chapter 7. The seismicity is very dense and localized during the injection operation. It is an important question how the seismicity may evolve with the injection/pumping, hoping that we are able to optimize the operation and minimize the related seismic hazard. The attempt presented by Maury et al. (2019) is a challenging topic. We learn that each injection step (change in injection flow and well pressure) may increase instantaneously the seismicity rate and this may decay with time gradually. This work will absolutely need further inputs and applications to verify the hypotheses of the model and establish the workflow. Figure 17 shows a more general example of the statistical analysis on the Oklahoma seismicity due to the waste water injections (Aochi et al., 2021). We learn that a small quantity of the injected fluid volume may trigger the seismicity, and its temporal evolution can be written with a function of volume and time.

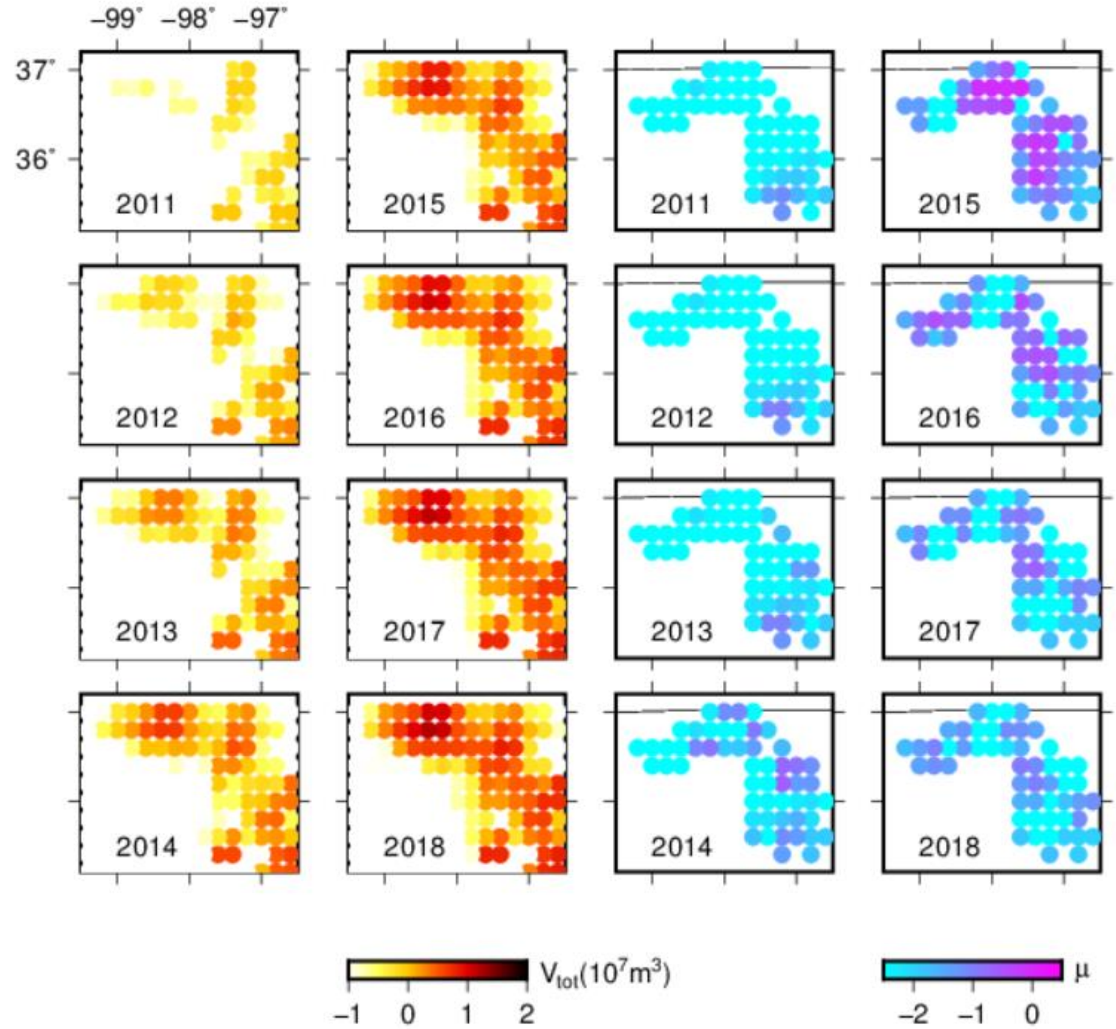

Figure 17: Statistical analysis of spatio-temporal evolution of injected fluid volume and seismicity rate every grids in the state of Oklahoma since 2011 (modified after Aochi et al., 2021).

13 RELEVANCE OF THIS STUDY TO THE NEW GREEN DEAL AND PROPOSED FUTURE STUDIES

The depleted reservoirs are the potential targets of the storage of gas and CO2, which are the requirements of sustainable energy and environment of the world. We will need to use them safely to reach our goal of CO2 reduction and to contribute to the climate change problem. The classical seismological study will always be necessary to monitor the safety of the area and the region. In the research, the area of visible seismicity is often emphasized. However, it is important to know that not all the injection wells induce seismicity (Figure 18). It is necessary to analyze globally the relation between the wells and (no) seismicity to bring a safer strategy for subsurface usage.

USGS Map of 21 Areas Impacted by Induced Earthquakes

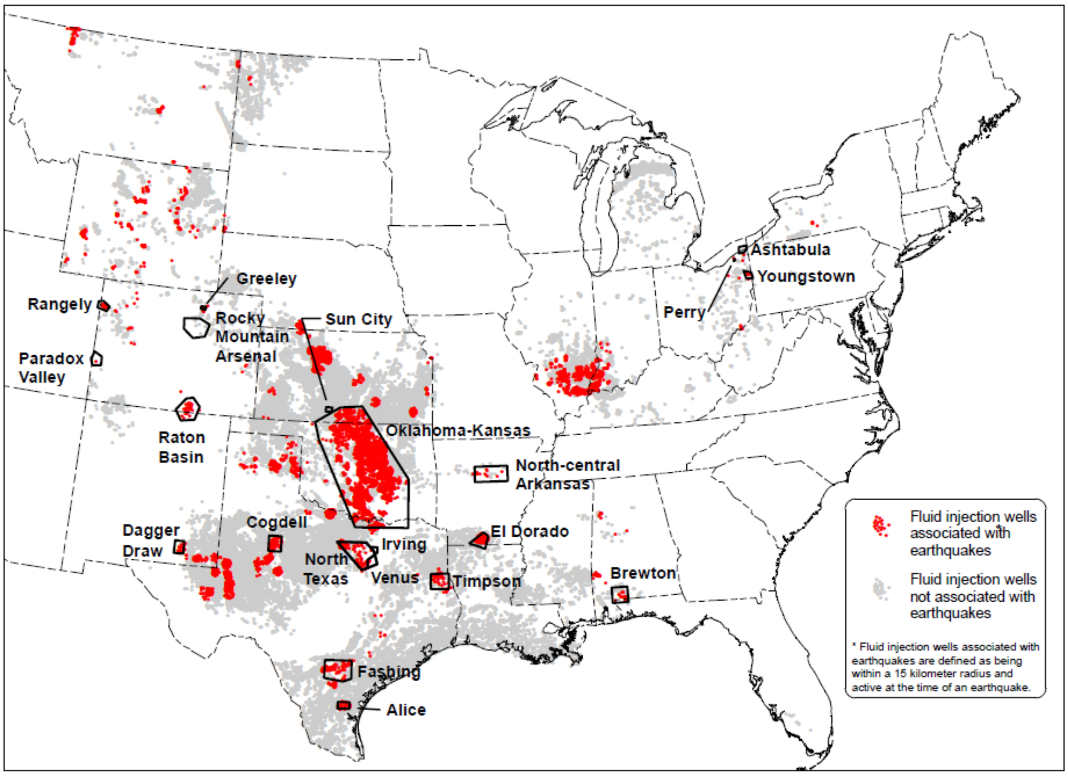

USGS map displaying 21 areas impacted by induced earthquakes as well as the location of fluid injection wells that have and have not been associated with earthquakes.

Figure 18 : USGS map displaying 21 areas impacted by induced earthquakes as well as the location of fluid injection wells that have and have not been associated with earthquakes. (source: https://www.usgs.gov/media/files/usgs-map-21-areas-impacted-induced-earthquakes)

14 REFERENCES

Aochi, H. and A. Burnol (2018). Mechanism of the ML4.0 25th April 2016 earthquake in southwest of France in the vicinity of the Lacq gas field, J. Seismol., 22, 1139-1155, doi: 10.1007/s10950-018-9758-5.

Aochi, H., J. Maury and T. Le Guenan (2021). How do statistical parameters of induced seismicity correlate with fluid injection? Case of Oklahoma, *Seismol. Res. Lett.*, 92, 2573-2590, 2021. https://doi.org/10.1785/0220200386

Aochi, H., T. Ulrich, A. Ducellier, F. Dupros, & D. Michea (2013). Finite difference simulations of seismic wave propagation for understanding earthquake physics and predicting ground motions: Advances and challenges, J. Phys: Conf. Ser., 454, 012010, doi: 10.1088/1742-6596/454/1/012010.

Bardainne, T., N. Dubos-Sallée, G. Sénéchal, P. Gaillot & H. Perroud (2008). Analysis of the induced seismicity of the Lacq gas field (Southwestern France) and model of deformation, Geophys. J. Int., 172, 1151-1162, doi:10.1111/j.1365-246X.2007.03705.x

Biteau, J.-J., A. Le Marrec, M. Le Vot & J.-M. Masset (2006). The Aquitaine Basin, Petroleum Geosciences,, 12(3) : 247-273, doi :10.1144/1354-079305-674.

Grasso, J.-R. & G. Wittlinger (1990). Ten years of seismic monitoring over a gas field, Bull. Seism. Soc. Am., 80(2): 450-473.

Grasso, J.-R., A. Karimov, D. Amorese, C. Sue & C. Voisin (2018). Patterns of reservoir-triggered seismicity in a low-seismicity region of France, Bull. Seism. Soc. Am., 108, 2967-2982, doi:10.1785/0120180172.

Korean government commission (2019). Summary report of the Korean Government Comission on relations between the 2017 Pohang earthquake and EGS project. Doi: 10.22719/KETEP-2019043001

Maury, J., H. Aochi, S. ben Rhouma and T. le Guenan (2019). Detecting seismicity rate variation using ETAS model for induced seismicity, AGU Fall Meeting 2019, S23E-0681.

Payre, X., C. Maisons, A. Marblé & S. Thibeau (2014). Analysis of the passive monitoring performance at the Rousse CO2 storage demonstration pilot, Energy Procedia, 63, 4339-4357, doi :10.1016/j.egypro.2014.11.469.

Ross, Z., Cochran, E. S., Trugman, D. T. and Smith, J. D. (2020) 3D fault architecture controls the dynamism of earthquake swarms, Science, 368, 1357-1361. Doi:10.1126/science.abb0779

Schoenball, M. & Ellsworth, W. L. (2017). A systematic assessment of the spatiotemporal evolution of fault activation through induced seismicity in Oklahoma and southern Kansas. J. Geophys. Res., 122, 10,189–10,206. https://doi.org/10.1002/2017JB014850.

Segall, P. J.-R. Grasso, & A. Mossop (1994). Poroelastic stressing and induced seismicity near the Lacq gas field, southwestern France, J. Geophys. Res., 99:15423-15438.

Schmittbuhl, J. Lengline, O. Lambotte, S. Gruberg, M. Doubre, C. Vergne, J. Cornet, F., and Masson, F. (2021) Induced and triggered seismicity from Nov 2019 to Dec 2020 below the city of Strasbourg, France, EGU General Assembly 2021, online, EGU21-8374. https://doi.org/10.5194/egusphere-egu21-8374

Thibeau, S., S. Chiquet, C. Prinet, & M. Lescanne (2013). Lacq-Rousse CO2 Capture and Storage demonstration pilot : Lessons learnt from reservoir modelling studies, Energy Procedia, 37, 6306-6316, doi : 10.1016/j.egypro.2013.06.559.